

# Transforming Earths

## Designing 3D printable materials for robotic earth architecture

Ofer Asaf<sup>1</sup>, Pavel Larianovsky<sup>2</sup>, Arnon Bentur<sup>3</sup>, Aaron Sprecher<sup>4</sup>

<sup>1,4</sup>Material Topology Research Lab, Faculty of Architecture & Town Planning, Technion – Israel Institute of Technology

<sup>2,3</sup>National Building Research Institute, Faculty of Civil & Environmental Engineering, Technion – Israel Institute of Technology

<sup>1</sup>ofer.asaf@campus.technion.ac.il <sup>2</sup>pavel@technion.ac.il <sup>3</sup>bentur@technion.ac.il

<sup>4</sup>asprecher@technion.ac.il

*This paper explores the potential of using different local earthen materials in robotic additive manufacturing workflow despite challenges arising from soil variability. We propose a method to design materials based on locally sourced soils for 3D printing, focusing on the physical and mineralogical characteristics of the soil and the rheological properties of the mixture. By tailoring mixtures for both extrusion and stability and correlating straightforward tests with laboratory data, we advance the adaptability of earth-based materials for 3D printing. Experiments with robotic 3D printing across five soils validate our approach, suggesting pathways for furthering earthen material use in digital fabrication and underscoring the importance of material design.*

**Keywords:** Earth Construction, 3D Printing, Soil, Recycled Aggregates, Robotic Fabrication

## INTRODUCTION

Earthen construction is attracting attention in digital architecture due to the sustainable attributes of earth - a widely available and cost-effective material with a low carbon footprint (Reyes *et al.*, 2018). This revival aligns with the broader trend towards sustainable construction practices where earthen material shows promise (Pacheco-Torgal and Jalali, 2012). In the realm of digital construction, the application of robotic additive manufacturing (AM) techniques with earthen materials is expanding the capabilities of architects and designers to create architectural edifices (Gramazio Kohler Research, 2020; Mario Cucinella Architects and WASP, 2021; Rael and San Fratello, 2019). Among the various digital fabrication methods developed, extrusion-

based AM, or 3D printing, has emerged as a primary focus of research (Gomaa *et al.*, 2022).

However, integrating earthen materials, which vary highly according to location, into 3D printing processes presents unique challenges. The inherent variability in soil physical and mineralogical composition demands an approach to material customization, balancing the rheological properties of the material at fresh state (Asaf *et al.*, 2023). This paper addresses these challenges by proposing a method for developing earthen-based materials tailored for architectural 3D printing. Our approach considers the distinct properties of each soil, aiming to enhance the adaptability and performance of earthen materials in robotic AM. This paper aims to aid architects, engineers, and designers in transforming earth into structures via robotic 3D

printing, paving the way for more sustainable and context-aware building practices.

## BACKGROUND AND LITERATURE REVIEW

Historically, earthen materials have been fundamental in architecture due to their ubiquity and unique hygrothermal properties (Minke, 2012). With the advent of digital fabrication, specifically additive manufacturing, increasing research is dedicated to incorporating these traditional materials within 3D printing workflows. Various AM techniques were described for using earthen materials in digital fabrication such as impact printing (Ming *et al.*, 2022) and binder jetting (Mitterberger, 2019). This paper focuses on methods for designing materials for extrusion-based 3D printing of viscous-like earthen materials. In addition, we lay some theoretical background on the basic physical and mineralogical properties of earthen materials and how these affect the material for 3D printing applications.

### Methods for Designing Earthen Materials for 3D Printing

Current literature on designing earthen materials for 3D printing has been advancing rapidly in recent years. Central in these methods are the rheological properties of the mix. Perrot *et al.* (2018) pioneered the articulation of earth-based 3D printing processing parameters and suggested incorporating bio-based polymer to increase the material's thixotropy (Perrot *et al.*, 2018). Joshi *et al.* (2021) further discussed the importance of rheology in 3D printing of earth and the factors affecting it (Joshi *et al.*, 2021). Biggerstaff *et al.* (2022) described the shape stability of biopolymer-earth mixtures as a function of their rheological properties (Biggerstaff *et al.*, 2022). These studies demonstrate the importance of understanding earthen mixtures rheology for fully controlling 3D printing processes. Nevertheless, literature on the effect of different earthen materials on these properties is scarce, demanding further exploration of the design of

earthen materials for 3D printing, considering their inherent variability.

### Rheological Properties for 3D Printing

Understanding the rheological properties of earthen materials in 3D printing is essential for a successful process (Roussel, 2018). These properties ensure the mixture can be transported through the pumping and extrusion systems and maintain layer stability once deposited. Ideal materials must flow easily under the printhead extrusion forces but solidify quickly upon deposition. This behavior is governed by the material reaching a specific shear stress (static yield stress), then transitioning into a dynamic state characterized by plastic viscosity and dynamic yield stress as described by the Bingham model. Low dynamic values facilitate smooth flow and extrusion, while a rapid increase in static yield stress upon deposition ensures structural stability. Essentially, these materials must be thixotropic, reducing viscosity under dynamic shear conditions for easy extrusion and quickly solidifying when static to maintain structure. For unstabilized earthen mixtures, this can be pursued by tailoring the particle grading and mineralogical composition.

### Particle Grading

Earth-based materials can be characterized by their particle size distribution. The three main ranges of particle sizes are sand (>50 microns), silt (50-5 microns), and clay (>5 microns), each contributing to a different property of the material. The effect of particle grading has been researched for earthen construction (Cuccurullo *et al.*, 2021) but not highly researched for 3D printing of earthen materials, demanding further elucidations. Nevertheless, it can be argued that increasing clay presence will increase the material's plasticity, viscosity, and shrinkage. In addition, clay presence is crucial for creating a lubrication layer during the pumping stage. Increasing coarse particles will increase the fresh material's rigidity due to inter-particle friction and restrict shrinkage and crack formation in hardened state.

### Mineralogical Characteristics

Bedrock, topography, and climate influence soil's mineralogical characteristics, impacting the fresh properties of the material for 3D printing and the properties of the final printed object.

First, it is essential to distinguish between clay and non-clay minerals. Non-clay minerals, including quartz, calcite, feldspar, and dolomite, generally absorb less water due to their chemical composition. These minerals contribute to the rigidity of the material in its fresh state and provide structural integrity in its hardened state. Conversely, clay minerals are highly water-absorptive. The strong physical bonds between the clay platelets induce the strength of the material, which acts as a binder. Clays also improve the mixture's plasticity, which is essential for the texture of the extruded material. Second, non-expansive clays like kaolinite and illite are preferred for 3D printing due to their lower water absorption rate compared to expansive clays like montmorillonite and bentonite. This reduces the required water content for achieving sufficient viscosity, minimizing shrinkage, cracking, and enhances strength stability by being less sensitive to humidity changes.

### MATERIALS AND METHOD

This study aimed to identify an easy-to-follow methodology for transforming earthen materials into architectural objects via robotic 3D printing. The workflow for designing a 3D printable mixture is outlined in Figure 1. This method was developed based on empirical testing conducted with five

earthen materials varying in particle grading and mineralogy. It is important to note that this study focused on unstabilized earthen materials and that the addition of stabilizers such as cement, biopolymer, lime, etc., will likely affect the rheology of the fresh material and therefore, will demand further articulation of mixture design method.

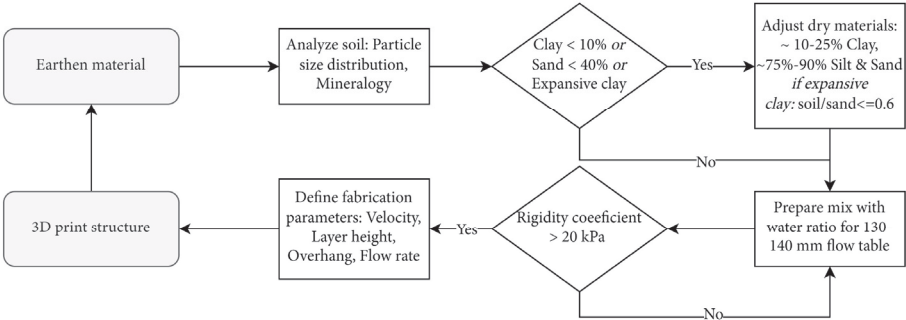
### Five Local Earthen Materials

Five unique local earthen materials were sourced from various localities across Israel. Ranging from north to south, the collected materials comprise: Rendzina soil from Kibbutz Afek (Rendzina), Terra-Rosa soil from Daly'at El Carmel (Terra-Rosa), Quarry sludge from Shufa quarry (Shufa), Loess Soil from the northwestern Negev (Loess), and Brown-clayey soil from Ramon Crater (Makhtesh Ramon). To tailor these materials for 3D printing applications, additional quartz sand and two types of local clays, Mamshit and Chocolate, were obtained from Agat Minerals Ltd. To avoid the presence of large particles of gravel and stone in the mix, the soils were submerged in water and left to homogenize for 24 hours. They were then filtered using a coarse 2.36 mm sift (US standard #8).

### Raw Material Characterization

The mineral and physical characteristics of each soil were determined by particle size distribution and XRD tests. The particle size distribution was characterized by two methods: a sedimentation test and a laser diffractometer.

Figure 1  
Workflow diagram  
for the preparation  
and 3D printing of  
earthen materials.



In the sedimentation test, a soil sample of approx. 300 gr was combined with water and non-foaming soap in a one-liter jar to promote the dispersion of fine clay particles. The sealed jar was then shaken vigorously to ensure thorough mixing. It was left to settle on a level surface, allowing particles to settle and form distinct layers—sand within 1-2 minutes, silt after one hour, and clay after 24 hours. The percentage of each particle type was calculated by measuring the sediment height at these specified intervals, providing a visual representation of the soil particle size distribution.

The particle-size distribution was analyzed using a laser diffractometer Mastersizer 3000 Particle Size Analyzer (Malvern Panalytical). A 0.1 g sample was mixed with 10 ml of isopropanol to avoid aggregation, followed by 30s of sonification. The mixture was slowly added to the Hydro LV device.

To analyze the mineralogical content, soils were micronized using a McCrone device, with samples ground at 1500 rpm for 15 minutes in the presence of isopropanol. X-ray diffraction was conducted with a PANalytical EMPYREAN diffractometer, utilizing a Cu-K $\alpha$  radiation source. Scans were performed from 5° to 70° in continuous mode, with Rietveld refinement for quantitative phase analysis.

Mixture Preparation

The mixtures were prepared using a high-shear pan mixer, starting with introducing all components into the mixer tank and then gradually adding water. Detailed ratios of the mix are outlined in Table 1. After incorporating the water, an initial mixing phase of 3 minutes ensured a uniform moisture

distribution. A subsequent inspection verified the absence of any unmixed dry ingredients, leading to a further 6 minutes of intensive high-shear mixing to achieve a homogenous mixture. After mixing, 50x50x50 mm cubes were prepared for visual inspection and evaluation of the mixtures, as seen in Figure 2.

Fresh Mixture Properties

The fresh properties of the mixtures were assessed for flowability and rigidity using a flow table and custom rigidity test, as described in Figure 3. These tests were developed to facilitate straightforward, low-cost methods for coarse evaluation of a mixture's rheological properties.

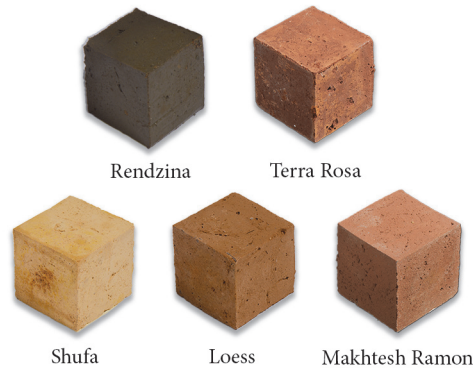


Figure 2  
Sample cubes for the earthen mixtures.

Annotation	Rendzina	Terra Rosa	Shufa	Loess	Makhtesh Ramon
Earth (kg)	38.3	80.0	34.3	44.7	30.7
Sand (kg)	38.3	x	48.9	42.1	57.1
Clay mamshit (kg)	x	x	2.6	x	x
Clay chocolate (kg)	x	10.0	x	x	x
Water (kg)	23.4	10.0	14.3	13.2	12.2

Table 1  
The composition of final earthen materials for a 100 kg mixture used for printing the specimens.

Figure 3  
Testing methods of  
the fresh mixture:  
A. flow table test  
and B. rigidity test.

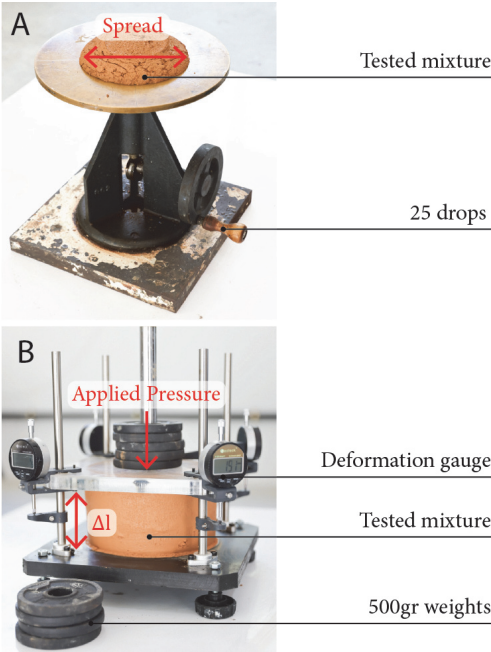
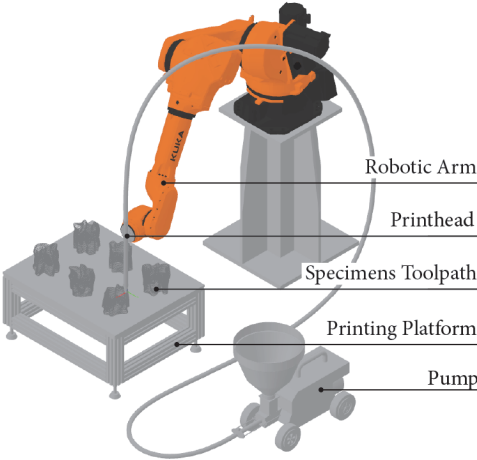


Figure 4  
3D printing robotic  
setup used in the  
printing of the  
specimens.



The flowability of the mixture was evaluated using a flow table test as seen in Figure 3A. This test utilizes the ASTM C230 flow table test, originally designed for hydraulic cement. A brass conical mold, positioned at the center of the table, was filled with the earthen mixture. Following the mold removal, the table underwent 25 jolts, enabling the measurement of the mixture spread.

The rigidity of the fresh green mixture was assessed utilizing the loading apparatus depicted in Figure 3B. A cylindrical mold with a diameter of 185 mm and a height of 100 mm was used for the test. The mold was filled in two stages with fresh material to ensure proper compaction, after which the mold was removed. A plate was placed on top the material and subjected to incremental manual loading of 500 g, up to an equivalent pressure of 6 kPa. The deformation at the four corners of the plate was measured, and the average deformation was recorded. This test allows for the creation of load-deformation curves from which the rigidity coefficient, defined as the slope of the curve, was calculated.

### Robotic 3D Printing Setup

The setup used in the study consisted of a KUKA KR50R2100 industrial robotic arm with a 50 kg payload and a 2100 mm reach. The printhead was a 450-mm-long metal rod with a 10-mm-diameter PET-G nozzle. The pumping system comprised of an MAI 2PUMP-PICTOR mortar pump for material flow, which was capable of a flow rate of 1.5-8.5 L/min, and was coupled with a concrete vibrator for consistent feed. The vibrator was found to be extremely important due to the narrow opening between the material reservoir and the pump screw. Flow rate control was achieved by adjusting the voltage of a GW Instek DC power supply. Material transportation between the pump and the printing head was done through a 5 m hose. The setup is described in Figure 4.

RESULTS AND DISCUSSION

Raw Material Analysis

Particle grading analysis is crucial for determining the suitability of earthen materials for 3D printing. Sedimentation testing and laser diffraction are two methods used to evaluate particle size distribution. Sedimentation testing estimates particle size based on settling velocity, while laser diffraction measures scattering of light to quickly and precisely gauge particle size.

From the results in Figures 5 and 6, it can be inferred that the sedimentation test provides a coarse understanding of particle grading, which is beneficial for developing 3D printing mixtures. It showed Loess, Terra Rosa, and Rendzina soil to be roughly aligned ( $R^2 = 0.89, 0.76, 0.60$ , respectively) with the diffraction test result. However, the Shufa soil ( $R^2 = 0.17$ ), being a quarry by-product with scant clay content, did not correlate well with sedimentation test results, which may be attributed to the differential settling rates of its predominantly non-clay spherical particles. Maktesh also did not with the diffraction test result ( $R^2 = 0.45$ )

Considering the mineralogical composition described in Figure 7, this characteristic is also pivotal to understanding the properties of the mixtures for 3D printing, serving as a complement to particle size distribution analysis. The analysis indicated that Rendzina and Loess soils contain substantial amounts of expansive clay minerals, namely montmorillonite, whereas Makhtesh Ramon soil predominantly comprises non-expansive kaolinite clay. Terra-Rosa and Shufa soils, on the other hand, consist primarily of non-clay minerals, namely quartz, and calcium carbonate.

The findings of the earthen materials analysis underscore the importance of employing both analyses to understand raw materials when formulating a 3D printing mixture comprehensively. The presence of expansive clay necessitates the addition of a more significant proportion of non-clay substances, such as sand, to mitigate shrinkage and improve mixture workability. Furthermore, while

earthen materials may display clay-sized particles, the absence of clay minerals means that a small amount of clay minerals should be incorporated in the mix to enhance the plasticity and workability of the material.

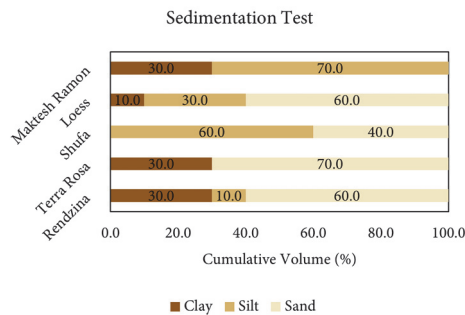


Figure 5  
Particle size distribution of the various soils based on sedimentation test.

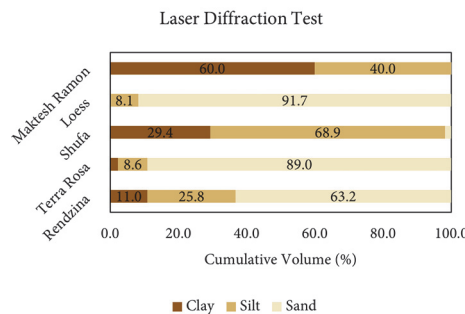


Figure 6  
Particle size distribution of the various earthen materials based on laser diffraction test.

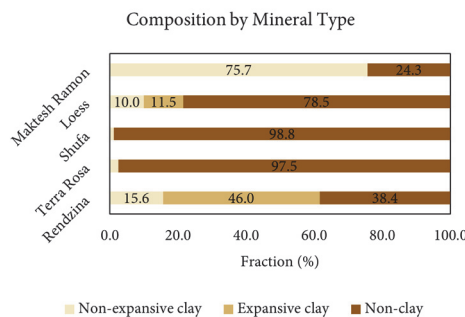


Figure 7  
Mineralogical composition of the various earthen materials.

Table 2  
Rigidity coefficient  
of the various  
earthen mixtures

Furthermore, while earthen materials may display clay-sized particles, the absence of clay minerals means that a small amount of clay minerals should be incorporated in the mix to enhance the plasticity and workability of the material.

**Design and Fresh Properties of the Mixtures**

The fresh properties of the mixtures were designed and evaluated following the method described in Figure 1.

With its high content of expansive clay minerals, the mix utilizing Rendzina soil demanded a large water content to reach adequate workability. Initially, the mixture was notably tacky and presented a rigidity coefficient lower than 10 kPa, which could result in plastic collapse even at low heights; adding sand and fine-tuning of the water content was necessary to achieve the desired flow and rigidity. Conversely, Terra Rosa soil, characterized by a high proportion of sand and a scant amount of clay, was amended with an additional 10% by weight of clay to enhance plasticity and texture. This soil required the lowest water quantity to attain the preferred flow. Shufa quarry byproduct, abundant in clay-sized particles yet deficient in clay minerals, was modified with sand and a small amount of clay to improve workability and plasticity. Loess soil posed considerable challenges, necessitating a significant inclusion of sand to procure a workable consistency and mitigate tackiness. Like Rendzina, Loess soil contains expansive clay, complicating the mixture's handling compared to non-expansive clay minerals. Lastly, Makhtesh Ramon soil, rich in kaolinite (76% by fraction), risks excessive shrinkage and cracking. Therefore, a substantial quantity of sand was incorporated during the mixture design. The final mixture designs are exhibited in Table 1.

The rigidity coefficient values of the mixtures, shown in Table 2, range between 20 and 67 kPa. No linear relationship was found between the mixture components, e.g., water or sand content, and the rigidity value. This suggests that a complex

relationship exists between these factors that determine this value. Still, lower values were found for Rendzina and Loess due to their expansive clay content requiring more water to balance the rheological properties.

Annotation	Rigidity Coefficient (kPa)
Rendzina	20.4
Terra Rosa	65.0
Shufa	39.2
Loess	22.0
Makhtesh Ramon	66.4

**Fabrication Parameters and Computational Design**

Tests were conducted to tailor the 3D printing process parameters for various earthen mixtures. When the pump was operated at 0.5 volts, the flow rate for all mixtures was reasonably uniform at approximately 1.2 l/m, setting a standard printing speed of 0.1 m/s. The optimal layer height was determined to be 5 mm, which provided the best balance between resolution and stability (Figure 8A); heights below this threshold led to inconsistent textures, while greater heights risked reducing layer-to-layer bonding, potentially destabilizing the structure. This resulted in a layer width of 15 to 20 mm and a maximum overhang angle of 40 degrees before the profile became convex (Figure 8B).

These experimentally derived parameters were then incorporated into a computational design workflow utilizing Grasshopper®. This process was employed to design a series of 1-meter-tall columns, each reflecting the unique characteristics of its corresponding earth type, inspired by the natural vegetation that thrives in each soil environment. The design protocol involved drafting section curves, generating lofted surfaces, assessing overhang tolerances, segmenting the model, and slicing it into layers for printing. The layers were visualized to inspect the final column shape (Figure 8C). Each segment's layers were divided into 5 mm

XY planes and translated into KRL code for robotic printing.

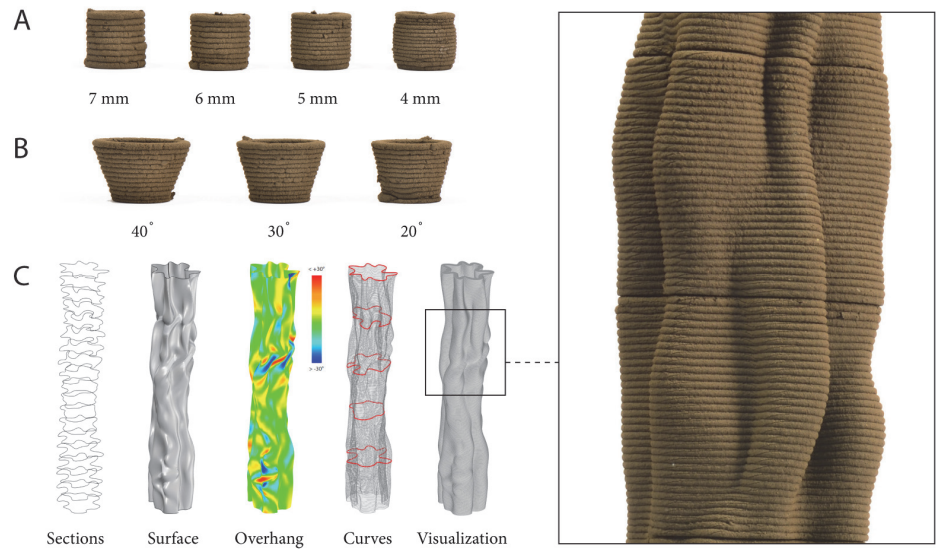


Figure 8  
A. Optimal layer height analysis. B. Overhang test. C. Computational design workflow, demonstrated for Rendzina soil. Work by students Kateryna Suzina, Gal Dayan and Siwar Naddaf.



Figure 9  
Five 1-meter columns 3D printed using the earthen materials examined in this study.



## **Fabrication of Five Columns**

To validate the method for designing earthen materials for 3D printing, five 1-meter columns were printed from the mixtures, as seen in Figure 9. The fabrication and the design of these columns were executed by a group of seventeen students taking part in a seminar at the Material Topology Research Lab at the Technion Faculty of Architecture and Town Planning. Each column was segmented into five or six sections to avoid plastic collapse and deformation of the structure. When printed, all the mixtures exhibited good behavior and texture, resulting in a model similar to the one designed computationally.

## **CONCLUSIONS**

This paper introduced a method for designing a 3D printable earth-based mixture that considers the physical and mineralogical properties of raw materials and their fresh-state properties. Our analysis of raw material characterization methods, comparing low-cost and high-end tests, suggests that sedimentation tests can reveal some insights into the earthen material particle grading, especially for soils rich in clay minerals. Nevertheless, this test is less efficient in estimating the particle grading for soils containing clay-sized particles, which are non-clay minerals. In addition, our results suggest the importance of considering both the grading and mineralogy of earthen materials for the design of earth-based materials for 3D printing.

Mixtures from five different soils were developed using the method described. The fresh properties were assessed using two testing methods that predict flow and rigidity. Five 1-meter columns were designed and printed using a robotic setup from the developed mixtures. The printed columns' texture and shape stability validate our method for designing materials that present the rheological properties required for the process.

Future research could aim at formulating methods for designing stabilized earthen materials for 3D printing to enhance their long-term

mechanical properties and durability, essential for their integration into the built environment. This could be achieved by incorporating mineral or biological stabilizing agents and fibers. Furthermore, this research lays the groundwork for exploring the broader implications of integrating earthen materials into architectural practice, including scalability, cost-effectiveness, and environmental considerations. Understanding the effect of the soil matrix on the short-term rheological properties is vital for a successful 3D printing process. Such advancements would contribute significantly to the use of earthen materials in architecture, combining the benefits of traditional materials with digital fabrication.

## **ACKNOWLEDGMENT**

The authors would like to thank the students who participated in the seminar Introduction to Architectural Robotics, which took place at the Faculty of Architecture and Town Planning: Almog Nezer, Arz Zaknoon, Eliad Michli, Gal Dayan, Juan Marjeh, Juman Abas, Kateryna Suzina, Maria Katzman, Netanel Lagziel, Ofri Dar, Ohad Meyuhas, Ruba Khalaily, Sherry Atare Khasdan, Sivan Shafrir, Siwar Naddaf, and Tair Shekel. Special thanks are reserved for Kateryna Suzina for her help in preparing materials and illustrations for this paper. We would also like to extend our gratitude to the Azrieli Foundation for its generous support enabling this study, and for Technion Material Topology Research Lab for contributing to the deployment of the experiments.

## **REFERENCES**

- Asaf, O., Bentur, A., Larianovsky, P. and Sprecher, A. (2023), "From soil to printed structures: A systematic approach to designing clay-based materials for 3D printing in construction and architecture", *Construction and Building Materials*, Elsevier, Vol. 408, p. 133783, doi: 10.1016/J.CONBUILDMAT.2023.133783.

- Biggerstaff, A., Lepech, M., Fuller, G. and Loftus, D. (2022), "A shape stability model for 3D printable biopolymer-bound soil composite", *Construction and Building Materials*, Elsevier, Vol. 321, p. 126337, doi: 10.1016/J.CONBUILDMAT.2022.126337.
- Cuccurullo, A., Gallipoli, D., Bruno, A.W., Augarde, C., Hughes, P. and La Borderie, C. (2021), "A comparative study of the effects of particle grading and compaction effort on the strength and stiffness of earth building materials at different humidity levels", *Construction and Building Materials*, Elsevier, Vol. 306, p. 124770, doi: 10.1016/J.CONBUILDMAT.2021.124770.
- Gomaa, M., Jabi, W., Soebarto, V. and Xie, Y.M. (2022), "Digital manufacturing for earth construction: A critical review", *Journal of Cleaner Production*, Elsevier, Vol. 338, p. 130630, doi: 10.1016/J.JCLEPRO.2022.130630.
- Gramazio Kohler Research, E.Z. (2020), "Clay Rotunda", <https://gramaziokohler.arch.ethz.ch/web/e/projekte/430.html>, 27 November.
- Joshi, A., Poullain, P., Craveiro, F. and Bártolo, H. (2021), "Earth as a Construction Material for Sustainable 3D Printing: Rheological Aspect", *International Conference of Progress in Digital and Physical Manufacturing*, Springer, pp. 270–280.
- Mario Cucinella Architects and WASP. (2021), "TECLA - Technology and Clay", <https://www.mcarchitects.it/tecla-2>, 23 February.
- Ming, C., Mirjan, A., Medina Ibáñez, J., Gramazio, F. and Kohler, M. (2022), "Impact Printing", *3D Printing and Additive Manufacturing*, Mary Ann Liebert Inc., Vol. 9 No. 3, pp. 203–211, doi: 10.1089/3dp.2021.0068.
- Minke, G. (2012), *Building with Earth: Design and Technology of a Sustainable Architecture*, Birkhäuser Basel, doi: <https://doi.org/10.1007/3-7643-7873-5>.
- Mitterberger, D. (2019), "Soil 3D Printing", *ACADIA 19:UBIQUITY AND AUTONOMY* (Proceedings of the 39th Annual Conference of the Association for Computer Aided Design in Architecture (ACADIA) ISBN 978-0-578-59179-7), The University of Texas at Austin School of Architecture, Austin, Texas, pp. 586–595.
- Pacheco-Torgal, F. and Jalali, S. (2012), "Earth construction: Lessons from the past for future eco-efficient construction", *Construction and Building Materials*, Elsevier, Vol. 29, pp. 512–519, doi: 10.1016/J.CONBUILDMAT.2011.10.054.
- Perrot, A., Rangeard, D. and Courteille, E. (2018), "3D printing of earth-based materials: Processing aspects", *Construction and Building Materials*, Elsevier Ltd, Vol. 172, pp. 670–676, doi: 10.1016/j.conbuildmat.2018.04.017.
- Rael, R. and San Fratello, V. (2019), "MUD FRONTIER: ARCHITECTURE AT THE BORDERLANDS", <http://emergingobjects.com/project/mud-frontiers-part-ii/>, October.
- Reyes, A.V., Gomaa, M., Chatzivasileiadi, A., Jabi, W. and Wardhana, N.M. (2018), "Computing Craft Early stage development of a robotically-supported 3D printing system for cob structures", *36th Annual Education and Research in Computer Aided Architectural Design in Europe (ECAADe)*, Lodz, Poland, pp. 17–21.
- Roussel, N. (2018), "Rheological requirements for printable concretes", *Cement and Concrete Research*, Pergamon, Vol. 112, pp. 76–85, doi: 10.1016/J.CEMCONRES.2018.04.005.